Organosilica Derivatives

DOI: 10.1002/ange.201104063

Periodic Mesoporous Organosilica Derivatives Bearing a High Density of Metal Complexes on Pore Surfaces

*Minoru Waki, Norihiro Mizoshita, Takao Tani, and Shinji Inagaki**

Periodic mesoporous organosilicas (PMOs) synthesized from alkoxysilane precursors bridged with organic moieties, $R[Si(OR')_3]_n$, $n \geq 2$, R = organic group, R′ = CH_3, C_2H_5, etc. by surfactant-directed self-assembly are a new class of functional materials that have well-defined nanoporous structures and highly functional organic groups in the silica walls.[1] It is preferable to incorporate organic groups in the pore walls rather than to graft them on the wall surfaces because in the former case the organic groups offer little resistance to the diffusion of molecules and ions in the mesochannels and are quite resistant to leaching. Many PMOs containing bridging organic groups (R) that range from aliphatic and aromatic hydrocarbons to heterocycles and metal complexes have been reported.[2,3] Incorporating metal complexes into PMO frameworks is particularly important because metal complexes possess unique features such as catalytic activity, luminescence emission, redox properties, and excited-state reactivity.[4]

PMOs with metal complexes are usually prepared by co-condensation of a metal-complex-bridged alkoxysilane precursor and a large amount (typically over 90%) of tetraethoxysilane. This is due to general difficulties in producing PMOs from just a precursor with a bulky metal complex because of weak interaction between hydrolyzed precursors and surfactants.[5] An alternative approach is to form metal complexes on a pore surface after synthesis by using bridging organic groups in the framework as metal ligands. Matsuoka and co-workers attached the organometallic fragments $\{Cr(CO)_3\}$ and $\{Mo(CO)_3\}$ to the phenyl ring of phenylene(Ph)-bridged PMO.[6] Recently, Polarz and co-workers reported the coordination of transition-metal cations to Ph–PMOs functionalized with carboxylic, dithiocarboxylic, acetylacetonate, and amine groups.[7] This approach has the advantage that bulky metal complexes can be densely and selectively integrated on the pore surface of highly ordered PMOs. However, these metal complexes attached to a PMO framework have limited functionalities mainly because of the poor ligand ability of these PMOs.

Recently, octahedral d^6 metal complexes such as polypyridine-coordinated ruthenium (Ru^{II}) and iridium (Ir^{III}) complexes have been attracting interest because of their photophysical properties and they have been widely utilized for dye-sensitized solar cells,[8] organic light emitting devices,[9] and photocatalysts.[10] Typical ligands for the d^6 metal complexes are bipyridine and 2-phenylpyridine (PPy).[11] Thus, the synthesis of PMO containing such chelating ligands in the framework is important for the formation of highly functional d^6 metal complexes on the pore surface.

Herein, we report the synthesis of a novel PMO containing PPy moieties in the PMO framework (PPy–PMO) and the successful formation of a high density of Ru or Ir polypyridine complexes on the pore surfaces (Scheme 1). The PPy ligands in the pore walls of the obtained PPy–PMOs exhibit molecular-scale periodicity, in which their molecular axes are aligned in parallel to the channel direction, with a high degree of freedom to rotate about the Si–C axis. The unique environment of the PPy ligands in the walls was found to realize efficient cyclometalation to form $[Ru^{II}(bpy)_2(ppy)]^+$ or $[Ir^{III}(ppy)_3]$ complexes by a post-synthesis treatment of PPy–PMO with metal complex precursors. PMOs with a high density of metal complexes on the pore surface have great potential in applications such as for efficient heterogeneous catalysts and sensors because the metal complexes hardly hinder the facile diffusion of molecules and ions in the mesochannels compared with conventional metal-complex-functionalized mesoporous silicas with organic linkers.

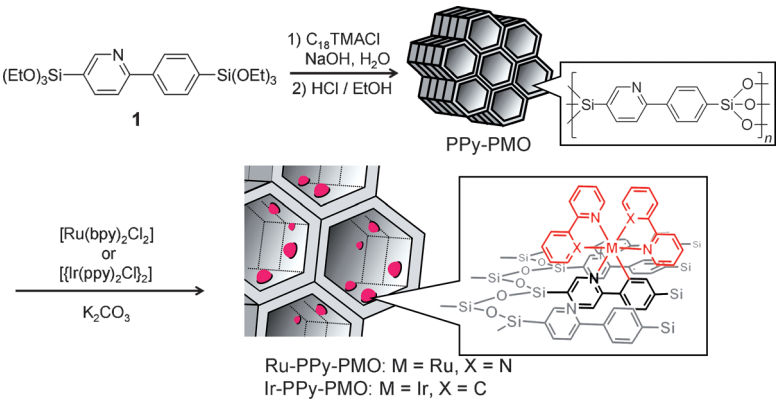

Scheme 1. Two-step synthesis of periodic mesoporous organosilicas (PMOs) with a high density of Ru and Ir polypyridine complexes on their pore surfaces.

The PPy-bridged alkoxysilane precursor, 2-(4-triethoxysilylphenyl)-5-triethoxysilylpyridine **1**, was synthesized from 2,5-dibromopyridine and 4-(trimethylsilyl)phenylboronic acid by a four-step reaction. The detailed procedure is described in the Supporting Information. PPy–PMO powder was obtained

[*] Dr. M. Waki, Dr. N. Mizoshita, Dr. T. Tani, Dr. S. Inagaki
Toyota Central R&D Labs., Inc., CREST/JST
Nagakute, Aichi 480-1192 (Japan)
E-mail: inagaki@mosk.tytlabs.co.jp

Supporting information for this article is available on the WWW under http://dx.doi.org/10.1002/anie.201104063.

by basic hydrolysis and polycondensation of the precursor in the presence of a cationic surfactant, octadecyltrimethylammonium chloride (C_{18}TMACl; Scheme 1). The surfactant was removed from the as-synthesized PPy–PMO by solvent extraction using a mixture of aqueous HCl and ethanol. The complete removal of the surfactant was confirmed by infrared absorption (IR) measurements (Figure S1 in the Supporting Information).

The X-ray diffraction (XRD) profile of the as-made PPy–PMO (Figure 1a, gray) contains a signal at a low scattering angle of $2\theta \approx 1.88°$ (d spacing of 4.7 nm), which suggests the

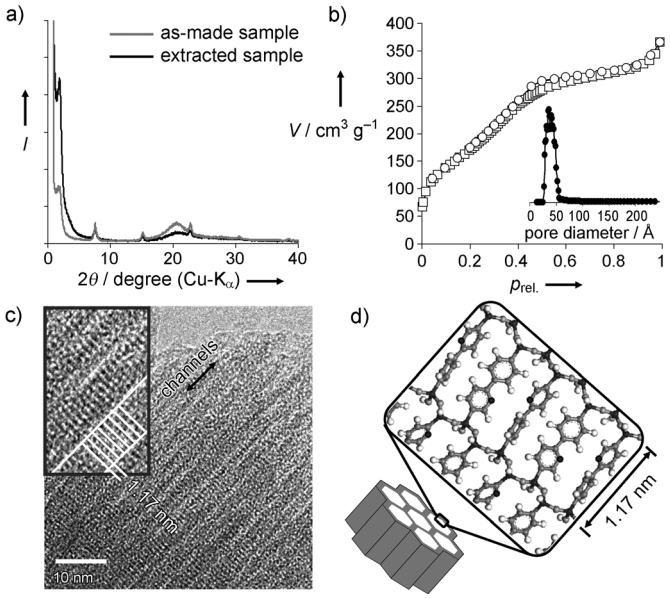

Figure 1. a) XRD profiles, b) nitrogen adsorption isotherms, c) transmission electron microscopy image, and d) structural model of PPy-PMO. Insets in (b) and (c) show DFT pore size distribution and an enlarged TEM image, respectively.

existence of a mesoscopically ordered structure. The XRD pattern also contained five other signals at medium scattering angles ($2\theta = 5$–$40°$) with d spacings of 1.17, 0.59, 0.39, 0.30, and 0.23 nm. These signals are assigned to a molecular scale periodicity of 1.17 nm and its higher-order reflections. The low- and medium-angle reflections remained after extracting the surfactant (Figure 1a, black). TEM observations revealed a bundle structure of one-dimensional channels with a periodicity of 4–5 nm and many lattice fringes with an interval of 1.1–1.2 nm running perpendicular to the mesochannels (Figure 1c). These results indicate that the PPy moieties in the walls are aligned with their molecular axes parallel to the channel direction to form alternating organic and silica belt-like layers with an interval of 1.17 nm (Figure 1d); this structure is similar to those of crystal-like PMOs with aromatic moieties such as benzene, biphenyl, divinylbenzene, napthalene, and divinylpyridine.[12] However, PPy–PMO is the first example of crystal-like PMO possessing a chelating ligand in the framework. The successful formation of crystal-like PPy–PMO enables us to fabricate highly functional d^6 metal complexes on the periodic pore walls. The nitrogen adsorption–desorption isotherms were type IV isotherms, typical of mesoporous materials (Figure 1b). The Brunauer–Emmett–Teller (BET) surface area was 649 $m^2 g^{-1}$, the pore volume was 0.39 $cm^3 g^{-1}$, and the DFT pore diameter was 3.7 nm. The pore wall thickness was estimated to be 1.7 nm from the structural parameters by assuming 2D hexagonal symmetry; this thickness corresponds to approximately four layers of the PPy moieties.

The solid-state ^{29}Si magic angle spinning (MAS) NMR spectrum of PPy–PMO showed two resonances at −71.3 and −80.9 ppm, which were assigned to T^2 and T^3 [T^n: $SiC(OH)_{3-n}(OSi)_n$] species, respectively, but no signals around −100 ppm because of Q^n [$Si(OH)_{4-n}(OSi)_n$] species (Figure S2A in the Supporting Information). The ^{13}C cross-polarization MAS NMR spectrum showed four resonances at 117, 125, 133, and 139 ppm, which are primarily in consistency with those of the precursor (Figure S2B in the Supporting Information). The IR spectrum showed absorption bands assignable to C=C and C=N of the PPy group (1352–1585 cm^{-1}), Si–C (1149 cm^{-1}), and Si–O (1030 cm^{-1}; Figure S1 in the Supporting Information). These results indicate that both the Si–C bonds and the PPy moieties are preserved during synthesis and extraction.

Cyclometalation of the PPy ligands in PPy–PMO was performed by heating PPy–PMO powder in an ethylene glycol solution of $[Ru(bpy)_2Cl_2]\cdot 2H_2O$ or a glycerol solution of $[Ir(ppy)_2Cl]_2$ in the presence of K_2CO_3 at 120 °C for 24 h and subsequent washing with solvents to remove any unreacted precursor (Scheme 1). The obtained powders are denoted Ru–PPy–PMO and Ir–PPy–PMO, respectively.

UV/Vis spectra of Ru–PPy–PMO showed new absorption bands at 372, 416, 497, and 550 nm in addition to the original band at 305 nm caused by PPy–PMO (Figure 2a, black). The new bands were assignable to metal-to-ligand charge transfer (MLCT) transitions, which have been previously observed for $[Ru^{II}(bpy)_2(ppy)]^+$ complexes.[13] For further confirmation, the UV/Vis spectrum was compared to that of a model complex, $[Ru^{II}(bpy)_2(TMS\text{-}ppy)]^+$, in which the PPy ligand was trimethylsilylated (TMS) at the *para*-positions, similar to the Ru complexes in Ru–PPy–PMO (Figure 2b); the spectra are similar to each other. In addition, the UV/Vis spectrum differs from that of the precursor, $[Ru(bpy)_2Cl_2]\cdot 2H_2O$, which contains only two absorption bands at 379 and 557 nm (Figure S3 in the Supporting Information). This result suggests that the precursor underwent a reaction during treatment with PPy–PMO. These results indicate the successful formation of the $[Ru^{II}(bpy)_2(ppy)]^+$ complex on the PMO surface through cyclometalation of the PPy ligands in the framework.

On the other hand, Ir–PPy–PMO exhibited broad absorption bands at longer wavelengths in addition to the original band at 305 nm (Figure 2c). The band at 380 nm corresponds to the ^{1}MLCT transition and the shoulder around 480 nm can be assigned to the ^{3}MLCT transition according to previous reports.[14] Ir–PPy–PMO showed a strong emission (phosphorescence) at 550 nm with a luminescence quantum yield of 0.03 (Figure 2d). The lifetime measurement indicated that the emission decayed with two time constants of 250 ns and 1.0 μs, respectively (Figure S4 in the Supporting Information). These

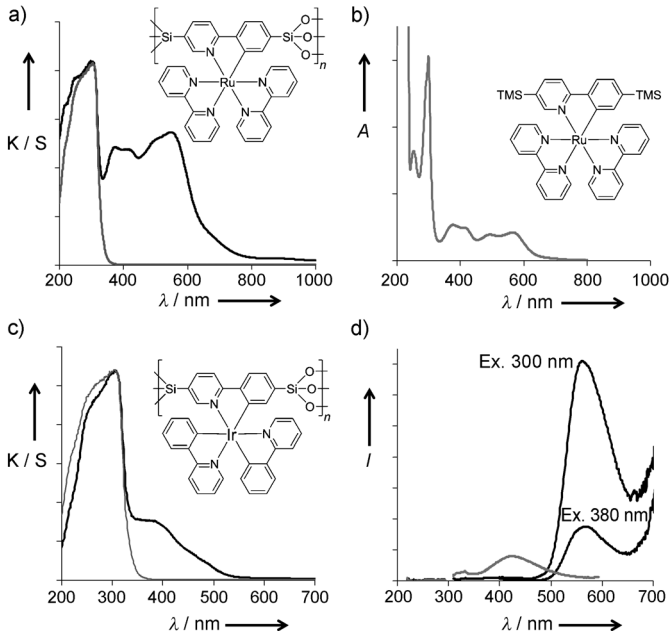

Figure 2. a) UV/Vis diffuse reflectance spectra of Ru–PPy–PMO (black) and PPy–PMO (gray) are depicted with Kubelka–Munk absorption coefficient (K/S); b) UV/Vis absorption spectrum of the model compound $[Ru(bpy)_2(TMS\text{-}ppy)]^+$ in CH_2Cl_2 (1.0×10^{-5} M); c) UV/Vis diffuse reflectance spectra of Ir–PPy–PMO (black) and PPy–PMO (gray); d) photoluminescence spectra of Ir–PPy–PMO excited at 300 and 380 nm (black) and of PPy–PMO excited at 300 nm (gray).

optical properties, such as the broad MLCT band shapes, the low quantum yield, and the short emission lifetime are typical for a meridional isomer of an $[Ir^{III}(ppy)_3]$ complex,[15] and are suggestive of the successful formation of $[Ir^{III}(ppy)_3]$ on the pore walls. The formation of the meridional isomer is reasonable because it is usually formed in low-temperature cyclometalation (< 140 °C).[16]

TEM observations confirm the preservation of the *meso*- and molecular-scale periodicities for both Ru–PPy–PMO and Ir–PPy–PMO, although XRD measurements indicate some reduction in the mesoscale structural order (Figure S5 and S6 in the Supporting Information). Nitrogen adsorption experiments reveal that the surface area and the pore volume of PPy–PMO decrease to 462–564 $m^2 g^{-1}$ and 0.26–0.31 $cm^3 g^{-1}$, respectively, during complex formation on the pore surface (Figure S5 and S6 in the Supporting Information). ^{29}Si and ^{13}C MAS NMR and IR spectra indicate the preservation of both Si–C bonds and PPy moieties during cyclometalation (Figure S7 in the Supporting Information).

The loaded amounts of Ru and Ir in Ru–PPy–PMO and Ir–PPy–PMO, respectively, were carefully determined by energy-dispersive X-ray spectroscopy (EDS), which was performed using an EDS attachment to the TEM system. EDS elemental analysis of many different areas on the Ru–PPy–PMO sample with various spot sizes (40–2500 nm) gave an atomic ratio Ru/Si of 0.05 (thus, Ru/PPy = 0.1) in almost all areas and Ru/Si = 0.04 or 0.06 in a few areas, which suggests that Ru was almost homogeneously distributed in the mesochannels (Figure S8 in the Supporting Information). Similarly, Ir/PPy = 0.02 was obtained for Ir–PPy–PMO (Figure S9 in the Supporting Information). Since the pore walls of PPy–PMO are composed of four PPy layers and only the outer two PPy layers (denoted by PPy*) are available for cyclometalation, Ru/PPy* and Ir/PPy* are 0.2 and 0.04, respectively. The lower amount of Ir than Ru may be due to the lower reactivity of $[Ir(ppy)_2Cl]_2$ with PPy ligands than $[Ru(bpy)_2Cl_2]\cdot 2H_2O$.[11b]

Figure 3a and b, respectively, show computer graphic images of the pore surface and the cross-section of the mesochannels for Ru–PPy–PMO, assuming that Ru/PPy* =

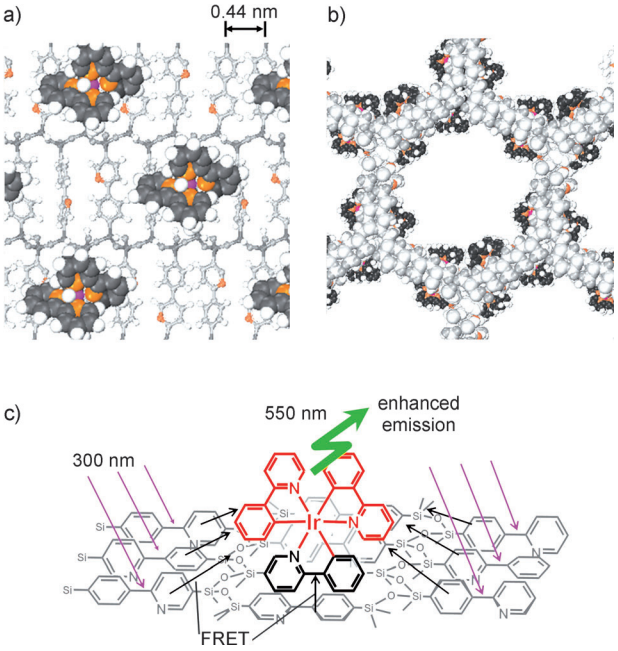

Figure 3. Computer graphic images of Ru–PPy–PMO; a) Ru complexes $[Ru^{II}(bpy)_2(ppy)]^+$ on pore surfaces of PPy–PMO with Ru/PPy* = 0.2; Ru complex and PPy–PMO are shown as CPK and ball-and-stick models; b) cross-section of a mesochannel in Ru–PPy–PMO; c) schematic image for light-harvesting of Ir–PPy–PMO.

0.2 and that the Ru complexes are homogeneously distributed. These figures indicate that the Ru complexes are densely accumulated on the pore surface and cause little pore blockage that would hinder diffusion of molecules and ions in the mesochannels. A molecular mechanics simulation of PPy–PMO reveals that the average PPy–PPy distance in the silicate layers is approximately 0.44 nm (Figure 3a), which is longer than the usual π–π stacking distance of aromatic compounds. Thus, the PPy moieties have a high degree of freedom to rotate about the Si–C axis, as pointed out by Sozzani and coworkers in their study of molecular rotors in Ph- and biphenyl-PMOs.[17] This high degree of rotational freedom of the PPy ligands may permit efficient cyclometalation with Ru complexes despite the PPy moieties being fixed in the rigid silicate framework.

Ir–PPy–PMO exhibited unique light-harvesting-antenna properties. The emission at 550 nm from $[Ir^{III}(ppy)_3]$ was greater for excitation at 300 nm than at 380 nm, as shown in Figure 2c. This result is thought to be caused by the more

efficient absorption of 300 nm light by the large amount of PPy moieties in the PMO framework and the light energy is transferred to the small amount of $[Ir^{III}(ppy)_3]$ complexes through Förster resonance energy transfer (FRET), which enhances emission relative to the emission due to direct excitation of the small amount of $[Ir^{III}(ppy)_3]$ by 380 nm light (Figure 3c). The almost complete quenching of the emission from the PPy moieties at 420 nm for Ir–PPy–PMO suggests efficient energy transfer from the PPy moieties to the $[Ir^{III}(ppy)_3]$ complex. The system presented is the first light-harvesting system for energy funneling into the acceptor (Ir complex) located on the pore walls, although we reported some PMO-based light-harvesting systems, in which acceptors such as dye molecules[18,19] and rhenium complexes[20] are placed in the mesochannels. Ru–PPy–PMO showed almost no emission because of the very low luminescence quantum yield of $[Ru^{II}(bpy)_2(ppy)]^+$. However, efficient energy transfer from the PPy moieties to $[Ru^{II}(bpy)_2(ppy)]^+$ should occur owing to an efficient overlap of the absorption band of $[Ru^{II}(bpy)_2(ppy)]^+$ with the emission band of PPy–PMO (Figure 2a and d). This result suggests that the antenna effect of PPy–PMO can enhance the photochemical properties of the Ru complex such as the redox property and the excited-state reactivity. The present light-harvesting systems with acceptors on the pore walls have the advantage that pore space can be fully utilized for further functionalization and as reaction fields.

In conclusion, novel crystal-like PPy–PMO was successfully synthesized. The PPy moieties in the pore walls were confirmed to function as ligands for cyclometalation, forming highly functionalized Ru^{II} and Ir^{III} complexes on the pore wall while maintaining the mesoporous structure. The Ru^{II} complexes are considered to be densely arranged on PPy–PMO, whereas Ir–PPy–PMO exhibited light-harvesting properties. The present PMOs can be further functionalized by incorporating functional molecules in the mesopores and/or coordinating other metal complexes. They are thus highly promising as a new class of functional hybrids and are suitable for constructing various photochemical and photophysical systems.

Experimental Section

General: All reagents and solvents were commercially available and were used without further purification. ^1H and ^{13}C NMR spectra were obtained using a Jeol ECX-400 spectrometer operating at 400 and 100 MHz, respectively. ^{29}Si dipolar decoupling (DD) and ^{13}C CP MAS NMR measurements were performed at 79.49 and 100.6 MHz, respectively, at a sample spinning frequency of 4 kHz using a Bruker Avance 400 spectrometer with a 7 mm zirconia rotor. For the ^{29}Si DD MAS NMR measurements, the repetition delay was 80 s and the pulse width was 4.5 μs. For the ^{13}C CP MAS NMR measurements, the repetition delay was 5 s, the contact time was 1.75 ms, and the pulse width was 4.5 μs (^1H 90° pulse). Chemical shifts were referenced to tetramethylsilane and glycine for ^{29}Si and ^{13}C NMR, respectively. XRD profiles were recorded on a Rigaku RINT–TTR diffractometer using $Cu_{K\alpha}$ radiation (50 kV, 300 mV). Nitrogen adsorption and desorption isotherms were measured using a Yuasa Nova3000e sorptometer. BET surface areas were calculated from the linear sections of BET plots ($P/P_0 = 0.1$–0.2). Pore-size distributions were calculated using the DFT method (DFT kernel: N_2 at 77 K on silica, cylindrical pores, nonlinear density functional theory (NLDFT) equilibrium model). Pore volumes were estimated by the t-plot method. TEM observations were performed using a Jeol JEM-EX2000 operating at 200 kV. IR spectra were collected on a Thermo Fisher Scientific Nicolet Avatar-360 FT-IR spectrometer using an attenuated total reflection (ATR) attachment. UV/Vis absorption and fluorescence emission spectra were obtained using Jasco V-670 and FP-6500 spectrometers, respectively.

Time-resolved phosphorescence measurements were performed using nanosecond 355 nm laser pulses by third-harmonic generation (THG) of a Nd^{3+}:YAG laser (Continuum, NY-81) for the excitation light source. The phosphorescence from the sample was focused on the slit of a monochromator (Ritsu, MC-10N). The output of the monochromator was monitored using an avalanche photodiode (Hamamatsu Photonics, S5343). The signal from the detector was recorded on a digital oscilloscope (Tektronix, TDS3032B). The entire system was controlled with a personal computer through a GP–IB interface. The observed decay curves were analyzed using commercially available software (Wave Metrics, IGOR Pro).

Ru–PPy–PMO: PPy–PMO (0.15 g) was added to a mixture of K_2CO_3 (0.62 g, 4.5 mmol), $[Ru(bpy)_2Cl_2]\cdot 2H_2O$ (0.23 g, 0.45 mmol), and ethylene glycol (15 mL) under an argon atmosphere. The suspension was stirred and heated at 120 °C for 24 h. The resulting precipitate was filtered and washed with DMSO and EtOH to remove any unreacted $[Ru(bpy)_2Cl_2]\cdot 2H_2O$, affording Ru–PPy–PMO.

Ir–PPy–PMO: PPy–PMO (0.15 g) was added to a mixture of K_2CO_3 (6.2 mg, 0.045 mmol), $[Ir(ppy)_2Cl]_2$ (0.015 g, 0.014 mmol), and glycerol (15 mL) under an argon atmosphere. The suspension was stirred and heated at 120 °C for 24 h. The resulting precipitate was filtered and washed with distilled water and $CHCl_3$ to remove any unreacted $[Ir(ppy)_2Cl]_2$, affording Ir–PPy–PMO.

Received: June 14, 2011
Revised: October 5, 2011
Published online: October 21, 2011

Keywords: mesoporous materials · metalation · phenylpyridine · sol–gel processes · solid-state structures

[1] a) S. Inagaki, S. Guan, Y. Fukushima, T. Ohsuna, O. Terasaki, *J. Am. Chem. Soc.* **1999**, *121*, 9611–9614; b) T. Asefa, M. J. MacLachlan, N. Coombs, G. A. Ozin, *Nature* **1999**, *402*, 867–871; c) B. J. Melde, B. T. Holland, C. F. Blanford, A. Stein, *Chem. Mater.* **1999**, *11*, 3302–3308.

[2] a) W. J. Hunks, G. A. Ozin, *J. Mater. Chem.* **2005**, *15*, 3716–3724; b) F. Hoffmann, M. Cornelius, J. Morell, M. Fröba, *Angew. Chem.* **2006**, *118*, 3290–3328; *Angew. Chem. Int. Ed.* **2006**, *45*, 3216–3251; c) S. Fujita, S. Inagaki, *Chem. Mater.* **2008**, *20*, 891–908.

[3] a) W. Wang, J. E. Lofgreen, G. A. Ozin, *Small* **2010**, *6*, 2634–2642; b) N. Mizoshita, T. Tani, S. Inagaki, *Chem. Soc. Rev.* **2011**, *40*, 789–800.

[4] a) *Applied Homogeneous Catalysis with Organometallic Compounds* (Eds.: B. Cornils, W. A. Hermann), VCH, Weinheim, **1996**; b) *Homogeneous Photocatalysis* (Ed.: M. Chanon), Wiley, New York, **1997**; c) *Transition Metal and Rare Earth Compounds III* (Ed.: H. Yersin), Springer, Heidelberg, **2004**.

[5] a) P. N. Minoofar, R. Hernandez, S. Chia, B. Dunn, J. I. Zink, A.-C. Franville, *J. Am. Chem. Soc.* **2002**, *124*, 14388–14396; b) C. Peng, H. Zhang, J. Yu, Q. Meng, L. Fu, H. Li, L. Sun, X. Guo, *J. Phys. Chem. B* **2005**, *109*, 15278–15287; c) B. Lei, B. Li, H. Zhang, S. Lu, Z. Zheng, W. Li, Y. Wang, *Adv. Funct. Mater.* **2006**, *16*, 1883–1891; d) E. Besson, A. Mehdi, C. Reyé, R. J. P. Corriu, *J. Chem. Mater.* **2006**, *16*, 246–248; e) J. Font, P. d. March, F. Busqué, E. Casas, M. Benitez, L. Teruel, H. García, *J. Mater. Chem.* **2007**, *17*, 2336–2343; f) E. Rossinyol, A. Prim, E. Pellicer,

J. Arbiol, F. Hernández-Ramírez, F. Peiró, A. Cornet, J. R. Morante, I. A. Solovyov, B. Tian, T. Bo, D. Zhao, *Adv. Funct. Mater.* **2007**, *17*, 1801 – 1806; g) L.-N. Sun, H.-J. Zhang, J.-B. Yu, S.-Y. Yu, C.-Y. Peng, S. Dang, X.-M. Guo, J. Feng, *Langmuir* **2008**, *24*, 5500 – 5507; h) Q. Yang, J. Liu, L. Zhang, C. Li, *J. Mater. Chem.* **2009**, *19*, 1945 – 1955; i) A. Zamboulis, N. Moitra, J. J. E. Moreau, X. Cattoën, M. W. C. Man, *J. Mater. Chem.* **2010**, *20*, 9322 – 9338; j) J. Huang, F. Zhu, W. He, F. Zhang, W. Wang, H. Li, *J. Am. Chem. Soc.* **2010**, *132*, 1492 – 1493; k) B. Karimi, D. Elhamifar, J. H. Clark, A. J. Hunt, *Chem. Eur. J.* **2010**, *16*, 8047 – 8053.

[6] T. Kamegawa, T. Sakai, M. Matsuoka, M. Anpo, *J. Am. Chem. Soc.* **2005**, *127*, 16784 – 16785.

[7] A. Kuschel, M. Luka, M. Wessig, M. Drescher, M. Fonin, G. Kiliani, S. Polarz, *Adv. Funct. Mater.* **2010**, *20*, 1133 – 1143.

[8] a) K. Kalyanasundaram, M. Grätzel, *Coord. Chem. Rev.* **1998**, *177*, 347 – 414; b) T. Bessho, E. Yoneda, J.-H. Yum, M. Guglielmi, I. Tavernelli, H. Imai, U. Rothlisberger, M. K. Nazeeruddin, M. Grätzel, *J. Am. Chem. Soc.* **2009**, *131*, 5930 – 5934.

[9] a) M. A. Baldo, S. Lamansky, P. E. Burrows, M. E. Thompson, S. R. Forrest, *Appl. Phys. Lett.* **1999**, *75*, 4 – 6; b) M. A. Baldo, M. E. Thompson, S. R. Forrest, *Nature* **2000**, *403*, 750 – 753; c) T. Tsutsui, M. Yang, M. Yahiro, K. Nakamura, T. Watanabe, T. Tsuji, Y. Fukuda, T. Wakimoto, S. Miyaguchi, *Jpn. J. Appl. Phys.* **1999**, *38*, L1502 – L1504.

[10] a) K. Kalyanasundaram, *Coord. Chem. Rev.* **1982**, *46*, 159 – 244; b) J. I. Goldsmith, W. R. Hudson, M. S. Lowry, T. H. Anderson, S. Bernhard, *J. Am. Chem. Soc.* **2005**, *127*, 7502 – 7510; c) A. Juris, V. Balzani, F. Barigelletti, S. Campagna, P. Belser, A. V. Zelewsky, *Coord. Chem. Rev.* **1988**, *84*, 85 – 277; d) D. A. Nicewicz, D. W. C. MacMillan, *Science* **2008**, *322*, 77 – 80; e) K. Okeyoshi, R. Yoshida, *Chem. Commun.* **2011**, *47*, 1527 – 1529.

[11] a) M. I. Bruce, *Angew. Chem.* **1977**, *89*, 75 – 89; *Angew. Chem. Int. Ed. Engl.* **1977**, *16*, 73 – 86; b) M. Albrecht, *Chem. Rev.* **2010**, *110*, 576 – 623.

[12] a) S. Inagaki, S. Guan, T. Ohsuna, O. Terasaki, *Nature* **2002**, *416*, 304 – 307; b) M. P. Kapoor, Q. Yang, S. Inagaki, *J. Am. Chem. Soc.* **2002**, *124*, 15176 – 15177; c) A. Sayari, W. Wang, *J. Am. Chem. Soc.* **2005**, *127*, 12194 – 12195; d) M. Cornelius, F. Hoffmann, M. Fröba, *Chem. Mater.* **2005**, *17*, 6674 – 6678; e) N. Mizoshita, Y. Goto, M. P. Kapoor, T. Shimada, T. Tani, S. Inagaki, *Chem. Eur. J.* **2009**, *15*, 219 – 226; f) M. Waki, N. Mizoshita, T. Tani, S. Inagaki, *Chem. Commun.* **2010**, *46*, 8163 – 8165.

[13] E. C. Constable, J. M. Holmes, *J. Organomet. Chem.* **1986**, *301*, 203 – 208.

[14] P. J. Hay, *J. Phys. Chem. A* **2002**, *106*, 1634 – 1641.

[15] a) W. J. Finkenzeller, H. Yersin, *Chem. Phys. Lett.* **2003**, *377*, 299 – 305; b) T. Kobayashi, N. Ide, N. Matsusue, H. Naito, *Jpn. J. Appl. Phys.* **2005**, *44*, 1966 – 1969.

[16] A. B. Tamayo, B. D. Alleyne, P. I. Djurovich, S. Lamansky, I. Tsyba, N. N. Ho, R. Bau, M. E. Thompson, *J. Am. Chem. Soc.* **2003**, *125*, 7377 – 7387.

[17] a) S. Bracco, A. Comotti, P. Valsesia, B. F. Chmelka, P. Sozzani, *Chem. Commun.* **2008**, 4798 – 4800; b) A. Comotti, S. Bracco, P. Valsesia, M. Beretta, P. Sozzani, *Angew. Chem.* **2010**, *122*, 1804 – 1808; *Angew. Chem. Int. Ed.* **2010**, *49*, 1760 – 1764.

[18] S. Inagaki, O. Ohtani, Y. Goto, K. Okamoto, M. Ikai, K. Yamanaka, T. Tani, T. Okada, *Angew. Chem.* **2009**, *121*, 4102 – 4106; *Angew. Chem. Int. Ed.* **2009**, *48*, 4042 – 4046.

[19] a) H. Takeda, Y. Goto, Y. Maegawa, T. Ohsuna, T. Tani, K. Matsumoto, T. Shimada, S. Inagaki, *Chem. Commun.* **2009**, 6032 – 6034; b) Y. Maegawa, N. Mizoshita, T. Tani, S. Inagaki, *J. Mater. Chem.* **2010**, *20*, 4399 – 4403.

[20] H. Takeda, M. Ohashi, T. Tani, O. Ishitani, S. Inagaki, *Inorg. Chem.* **2010**, *49*, 4554 – 4559.

